3D Microperiodic Hydrogel Scaffolds for Robust Neuronal Cultures

Jennifer N. Hanson Shepherd, Sara T. Parker, Robert F. Shepherd, Martha U. Gillette, Jennifer A. Lewis, and Ralph G. Nuzzo**

Three-dimensional (3D) microperiodic scaffolds of poly(2-hydroxyethyl methacrylate) (pHEMA) have been fabricated by direct-write assembly of a photopolymerizable hydrogel ink. The ink is initially composed of physically entangled pHEMA chains dissolved in a solution of HEMA monomer, comonomer, photoinitiator and water. Upon printing 3D scaffolds of varying architecture, the ink filaments are exposed to UV light, where they are transformed into an interpenetrating hydrogel network of chemically cross-linked and physically entangled pHEMA chains. These 3D microperiodic scaffolds are rendered growth compliant for primary rat hippocampal neurons by absorption of polylysine. Neuronal cells thrive on these scaffolds, forming differentiated, intricately branched networks. Confocal laser scanning microscopy reveals that both cell distribution and extent of neuronal process alignment depend upon scaffold architecture. This work provides an important step forward in the creation of suitable platforms for *in vitro* study of sensitive cell types.

1. Introduction

Mammalian tissue consists of intricate matrices of individual cells that receive complex chemical, electrical, and topographical cues from their 3D *in vivo* environment.[1] Yet standard *in vitro* cell culture methods rely on two-dimensional (2D) substrates that are poor mimics of real tissue environments.[2–4] This deficiency is especially relevant to brain tissue, where neurons exchange critical information across synapses and the 3D organization of neurons and their supporting cells is critical for function.[5] It is widely known that neuronal cells are influenced by their surrounding microenvironment; for example, process orientation is guided by both topographical[6–8] and chemical cues.[9–11] Nevertheless, most prior studies of neuronal cells have focused on planar or semi-planar[12] environments despite the important biological differences in 3D systems.[13–16]

The interactions of neuronal cells on structured 2D substrates was recently reported by Hanson *et al*.[8] They observed hippocampal neuron process outgrowth on post array topographies and identified two distinct response regimes. For post arrays with feature sizes of 10–20 μm, regular, aligned neuronal networks developed, while process wrapping around individual posts dominated on arrays of larger feature size (up to 200 μm)[8] Importantly, process outgrowth could be directed on both small and large scales though in fundamentally different ways.

To date, few 3D neuronal cell studies have been carried out and most have used bulk hydrogels with a randomized structure. For example Holmes *et al*.,[15] developed a fabrication method to create self-assembled peptide based scaffolds for the culture of PC12 cells, as well as primary rodent neurons, while Irons *et al*.[16] used disks of Matrigel to co-culture cerebral cortex neurons with astrocytes to conduct developmental and electrophysiological studies. In another effort, Moore *et al*.[17] used poly(2-hydroxyethyl methacrylate)/polylysine gels with a gradient of a neurotrophic factor to study dorsal root ganglia development. The prepolymer solution and initiator were cast into a glass tube and cured to produce a bulk pHEMA gel for their cellular study. While neuronal cells were able to integrate within these bulk matrices to varying degrees, their development in response to specific 3D architectural features could not be elucidated. Quite recently, Seidlits *et al*. used multiphoton excitation to pattern 3D protein features within a bulk methacrylated poly(hyaluronic acid)/N-vinylpyrrolidinone gel, subsequently modifying them to present IKVAV peptide sequences, and investigated the outgrowth and migration of dorsal root ganglia and hippocampal progenitor cells.[18] Embedded protein features of defined microperiodicity could be produced by this approach, however only limited cellular integration was observed. New biocompatible scaffolds with precisely controlled architectures are therefore needed to understand how organized 3D environments affect neuronal development.

J. N. Hanson Shepherd, S. T. Parker, R. F. Shepherd,
Prof. J. A. Lewis
Department of Materials Science and Engineering
University of Illinois at Urbana-Champaign
Urbana, Illinois, 1304 W Green St., Urbana, IL 61801, USA
Email: jalewis@illinois.edu
Prof. M. U. Gillette
Department of Cell and Development Biology
University of Illinois at Urbana-Champaign
601 South Goodwin Ave., Urbana, IL 61801, USA
Prof. R. G. Nuzzo
Department of Chemistry
University of Illinois at Urbana-Champaign
Urbana, Illinois, 505 South Mathews Ave., Urbana, IL 61801, USA
Email: r-nuzzo@illinois.edu

DOI: 10.1002/adfm.201001746

Here, we create 3D microperiodic pHEMA scaffolds by direct-write assembly[19–20] and investigate their effects on the development of primary rat hippocampal neurons. Towards this objective, a new hydrogel ink is developed that is composed of physically entangled pHEMA chains dissolved in HEMA monomer, comonomer, photoinitiator and water, which is photopolymerized upon printing to yield robust 3D scaffolds. This ink offers enhanced biocompatibility relative to its polyacrylamide-based counterpart recently introduced for patterning 3D scaffolds.[21] Using this approach, 3D pHEMA scaffolds of varying microperiodicity are patterned and cultured with primary rat hippocampal neurons and imaged in three dimensions with confocal laser scanning microscopy (CLSM). Through image analysis, we show that neuronal network development and cellular distribution within these 3D scaffolds is strongly influenced by their architecture.

2. Results and Discussion

To enable scaffold patterning, we designed a hydrogel ink that contains high molecular pHEMA chains dissolved in a photocurable solution composed of HEMA monomer, comonomer, photoinitiator, and water. The precise molecular weights and their respective concentrations of these long-chain pHEMA species are chosen to reside in a physically entangled state (**Figure 1**a), which greatly enhances ink viscosity under typical printing conditions. We determined that an optimal ink formulation composed of 25 wt% pHEMA (M_w 300 000) and 10 wt% pHEMA (M_w 1 000 000) enables the printed features to both retain their filamentary shape and span gaps in the underlying layer(s).[21]

This pHEMA-based ink possesses a low-shear viscosity, η_0, of ~180 Pa·s (see Figure 1b). Above a critical shear rate, $\dot{\gamma}_c \sim 10^{-1}$ s^{-1}, the ink displays pronounced shear thinning behavior as the physically entangled pHEMA chains align in response to the applied shear stress. In this regime, the ink viscosity can be fit to a power law ($\eta\dot{\gamma}^{n-1}$), yielding a shear thinning exponent n of 0.56, as indicated in Figure 1b. We can estimate the shear rate experienced by the ink at the nozzle walls during printing by:[22]

$$\dot{\gamma}_{wall} = \left(\frac{3+b}{4}\right)\frac{4Q}{\pi R^3} \quad (1)$$

where b is the inverse of the shear thinning exponent n, Q is the volumetric flow rate ($= v\pi R^2$), v is the print speed, and R is the nozzle radius. By using $n \sim 0.56$ and $b \sim 1.78$, the maximum shear rate applied at the nozzle walls during printing is estimated to be $\dot{\gamma}_{wall} \sim 420$ s^{-1}. At this shear rate, the ink viscosity is ~12 Pa·s, more than an order of magnitude below its zero shear plateau value, and it flows smoothly through the micronozzle during printing.

To enable printing of 3D microperiodic scaffolds, the ink filaments must span gaps in the underlying layers with minimal deformation. The ink elasticity is therefore another important rheological parameter that must be optimized. The shear elastic modulus (G') and viscous modulus (G'') of the pHEMA ink are shown in Figure 1c. The ink possesses a plateau elastic modulus (G') of ~120 Pa and a yield stress of ~330 Pa. At an oscillatory

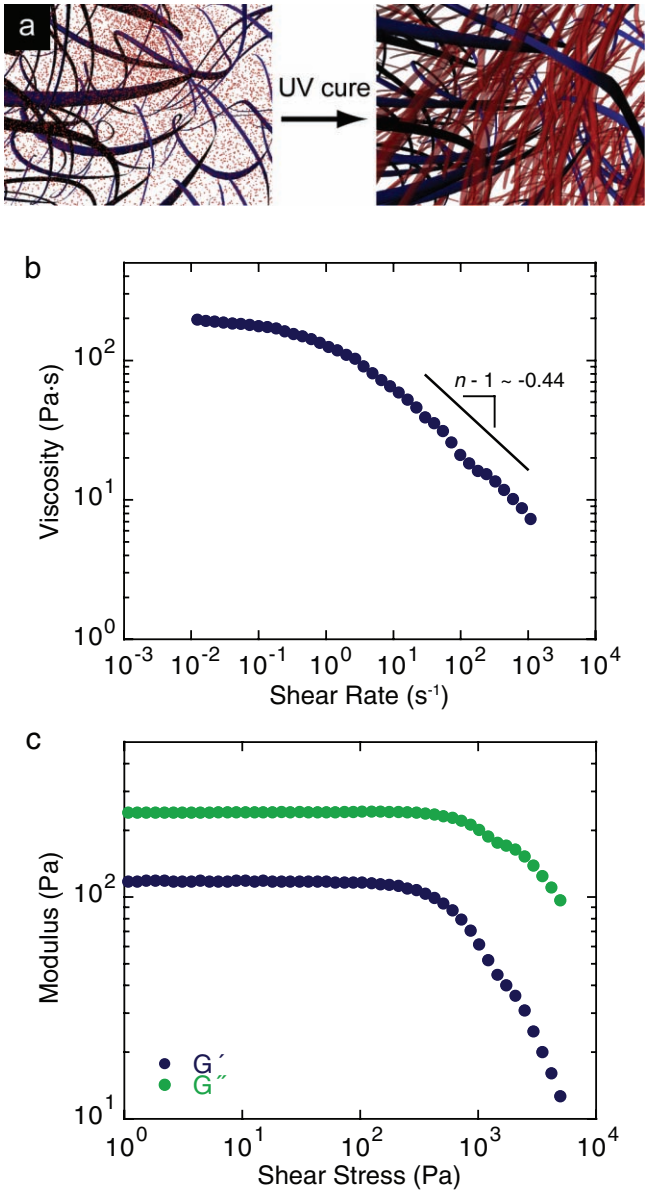

Figure 1. Structure and rheological behavior of pHEMA ink. (a) Schematic illustration of pHEMA ink before and after photopolymerization; blue chains represent physically entangled, high molecular weight species and red chains represent chemically cross-linked species (b) Ink viscosity as a function of shear rate; solid black line denotes the shear thinning exponent. (c) Ink shear elastic (G') and viscous (G'') moduli measured in oscillatory mode at 1 Hz.

frequency of 1 Hz, the ink displays a liquid-like response, i.e., $G'' > G'$, over all shear stresses probed experimentally, although the magnitudes of these two parameters are nearly identical. As the ink exits the nozzle, its elasticity should be rapidly enhanced due to drying, which further promotes shape retention of the patterned filaments prior to photopolymerization. Upon UV curing, chemically cross-linked pHEMA chains form, which interpenetrate their physically entangled counterparts. Concomitantly, the ink elasticity increases by three orders of magnitude to $G' \sim 10^5$ Pa (Figure 1a).

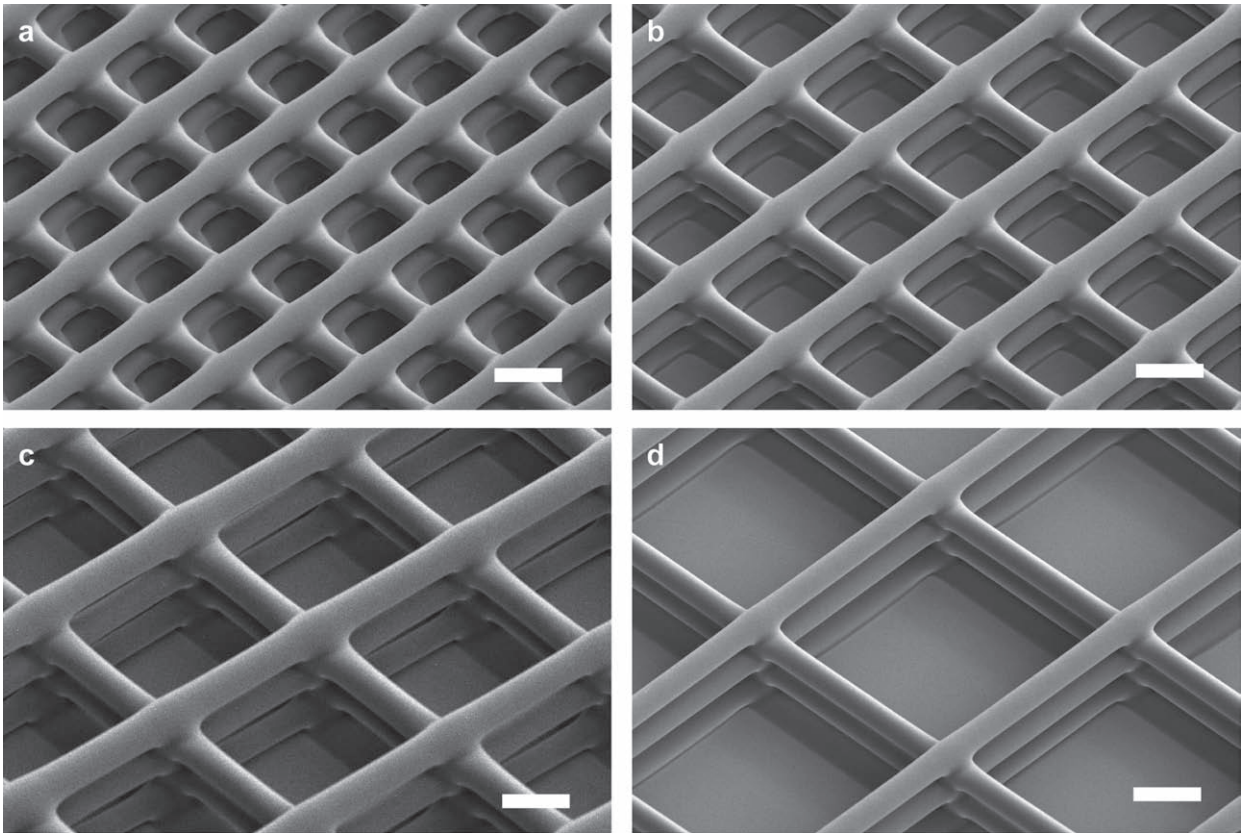

Figure 2. SEM micrographs of 3D pHEMA scaffolds of varying architecture, with pitch of a) 30 μm, b) 40 μm, c) 60 μm, and d) 80 μm. All scale bars are 20 μm.

3D microperiodic scaffolds of varying architecture are patterned by extruding this pHEMA-based ink through a 10 μm glass microcapillary nozzle into a predetermined pattern of orthogonally aligned filaments. Four scaffold architectures are produced; each of which contains orthogonal arrays of cylindrical hydrogel filaments, or rods, (ca. 10 μm in diameter) with a varying center-to-center spacing between adjacent rods of 30, 40, 60, and 80 μm (see **Figure 2**). The 3D hydrogel scaffolds contain fully interconnected porous networks and are able to survive immersion in aqueous culture solution for several days. To render the scaffolds growth compliant for primary rat hippocampal neurons, they are chemically modified by immersion in a polylysine solution,[23] where rapid absorption of these polypeptide species occurs (see Supporting Information, Figure S1).

After sterilization and subsequent treatment with unlabeled polylysine, the 3D hydrogel scaffolds are plated with postnatal day 1 primary rat hippocampal neurons. After seven days *in vitro*, the cultured neurons form extensive differentiated networks within the 3D scaffolds, as shown in the reconstructed CLSM images in **Figure 3** and in lower magnification images provided in Supporting Information, Figure S2. From these images, we find that the neuron response is dependent upon the scaffold architecture. As the spacing between adjacent patterned rods increases, there is a decrease in the number of cell somata that are fully integrated throughout the 3D scaffold and an increase in the number of neuronal networks established on the underlying glass substrate. The cell survival in each scaffold is high and the cultures develop stably without evidence of cell division. At seven days *in vitro*, cells show elaborate processes that exhibit MAP2, a protein commonly present in dendrites (see Supporting Information, Figure S3).

Figure 3 shows a top view of each 3D scaffold highlighting neuronal process organization, as well as a reconstructed side view illustrating cell distribution along the vertical direction. For scaffolds with a pitch of 30 μm, the majority of cell somata and their respective processes are confined to the top layers of the scaffold (Figure 3a). The neuronal processes clearly follow along the scaffold rods, which is expected given that hippocampal neurons preferentially attach to and follow along planar surface topographies, such as those formed by patterned post arrays.[8] As the scaffold pitch increases to 40 μm, the neurons create highly branched and aligned networks where the cell bodies are well distributed within the vertical dimension (Figure 3b). On this scaffold, the neuronal processes are able to penetrate all layers, instead of being confined to those near the top. When the scaffold pitch is further increased to 60 μm, the open pore channels are large enough to facilitate the partitioning of cells to lower layers, where they attach to the underlying substrate (Figure 3c). On these scaffolds, however, three-dimensionally supported neuronal networks do develop. As the pitch is increased further to 80 μm, the dominant somata response is the formation of intricate neuronal networks on

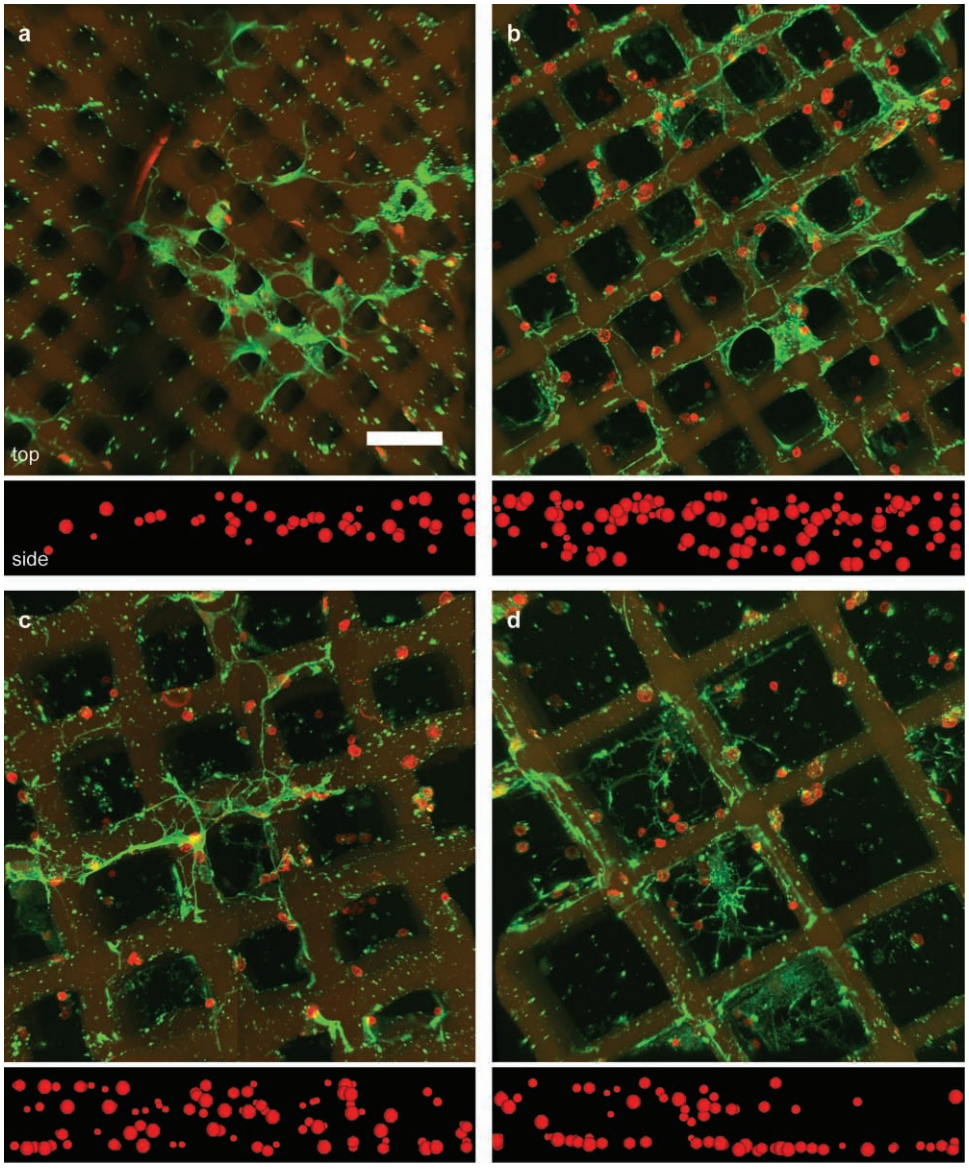

Figure 3. Confocal images (*x*-*y* scans, tiled) of primary rat hippocampal cells distributed within scaffolds of varying pitch: (a) 30 μm, (b) 40 μm, (c) 60 μm, and (d) 80 μm. A primary monoclonal antibody for actin is used to label the processes (green), while TO-PRO3 was used to label nuclei (red). Side view reconstructions schematically denote the positions (in *x*-*z* plane) of the neuronal somata, while their relative size indicates their position along the *y*-axis. Scale bar, 40 μm.

the underlying substrate surface (Figure 3d). Typically, these networks consisted of 1–2 neurons in each compartmentalized "pore" space with cellular processes that interact and densely follow the contours of the overlaying scaffold rods.

The cell soma distribution is quantitatively assessed as a function of lateral and vertical position (**Figure 4**) by 3D image analysis of confocal scans acquired in a representative volume of 250 × 250 × ~50 μm^3 within each scaffold. While the cells are well distributed laterally (Figure 4a), the pitch between filaments determines their vertical distribution in these scaffolds (Figure 4b). At the smallest pitch of 30 μm, the distribution is somewhat skewed to the upper layers of the scaffold (Figure 4b). In this architecture, the characteristic pore size is ~20–22 μm, which may hinder the ~10 μm somata from efficiently integrating deep within the scaffold. In scaffolds with a 40 μm pitch (~30–32 μm pores), the cell soma are well integrated vertically, while they tended to segregate to the region near the substrate in scaffolds with a pitch of either 60 or 80 μm.

To probe specific cell morphologies and process outgrowth behavior, individual cells are isolated and reconstructed in 3D through image analysis. Confocal images and reconstructions of representative cells are shown in **Figure 5**. The neuronal soma in Figure 5a displays a pyramidal morphology, which is commonly present in *in vitro* cultures of hippocampal neurons.[24] This 3D reconstruction reveals that the neuronal process follows underneath the scaffold on one side, while navigating over the top of the scaffold rod on the other. In Figure 5b, a cell body is seen to attach horizontally to the scaffold while

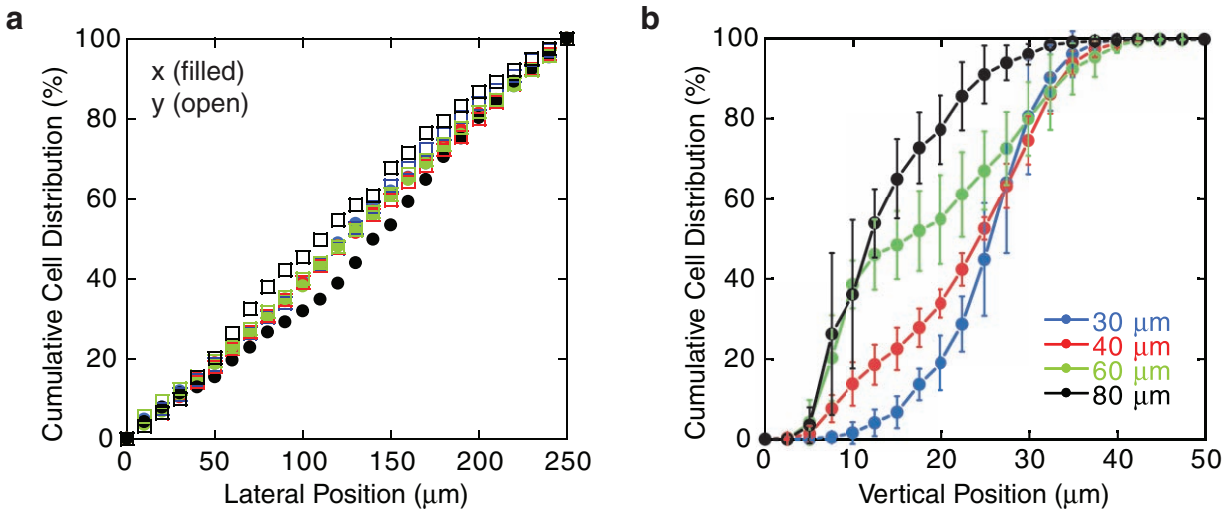

Figure 4. Cell distribution as a function of (a) lateral and (b) vertical position within 3D scaffolds of varying pitch.

its processes wrap around the adjacent rod in a high symmetry that maximizes multi-rod surface contacts. The inset reveals the process wrapping more clearly in a cross-sectional view. This behavior is most commonly observed on the topmost layers of scaffolds with the three smallest pitch sizes, where the neuronal processes can more easily access and interact with the entire circumference of the printed hydrogel rods. Somata with a distorted cell shape are also observed as they fit themselves between scaffold layers (see Supporting Information, Figure S4), highlighting a strong preference for interaction with the scaffold surface.

While it appears that the majority of cell bodies prefer to interact with these 3D scaffolds, some somata are vertically suspended with only their neuronal processes providing the necessary anchorage to the scaffold (Figure 5c). This suggests rapid attachment of neuronal cells to the hydrogel rods after plating onto the scaffold structures. An interesting morphology is revealed in this image where, instead of wrapping around an individual hydrogel rod, the process wraps around junctions formed at orthogonal intersections between printed rods in adjacent layers (a behavior most typically observed on scaffolds of the two smallest pitch sizes). Broader contact guidance along

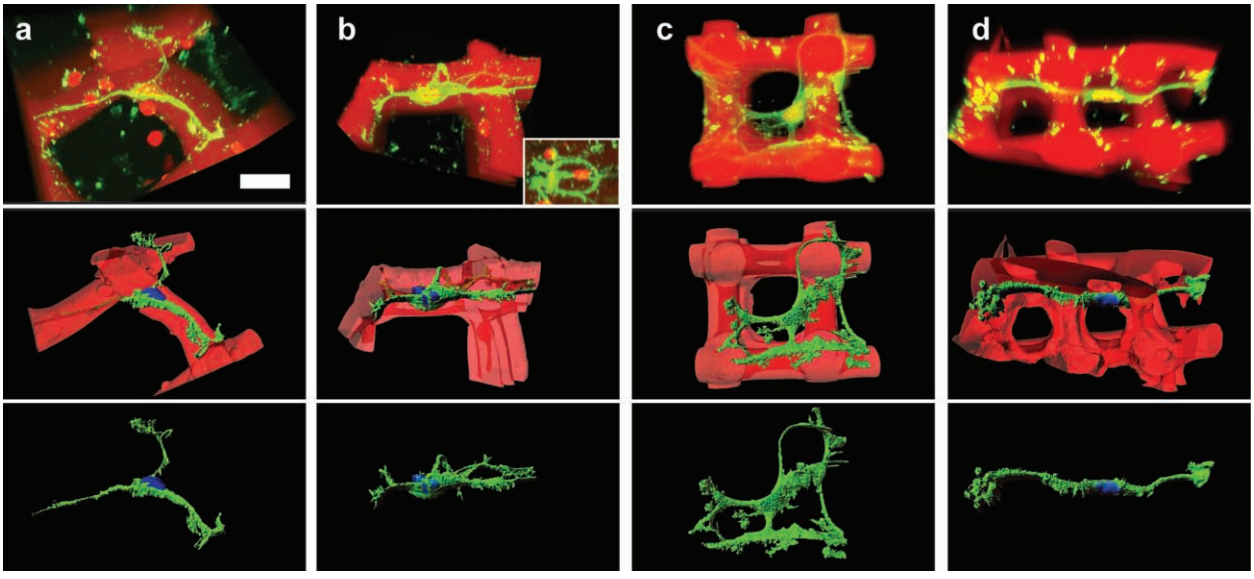

Figure 5. Confocal images of representative neuronal cells on the scaffolds (top row), reconstructed views (middle row) and reconstructed view of cells only (bottom row). (a) Pyramidal soma morphology on scaffold (60 μm pitch). (b) Neuronal process wrapping around cylindrical feature within scaffold (60 μm pitch). (c) Soma supported by neuronal processes on scaffold (40 μm pitch). (d) Process contact guidance on a scaffold (30 μm pitch). In the confocal images, the scaffold and cell nuclei are stained red and the processes are green. In the reconstructions, nuclei are colored blue, while actin is colored green. Scale bar, 20 μm.

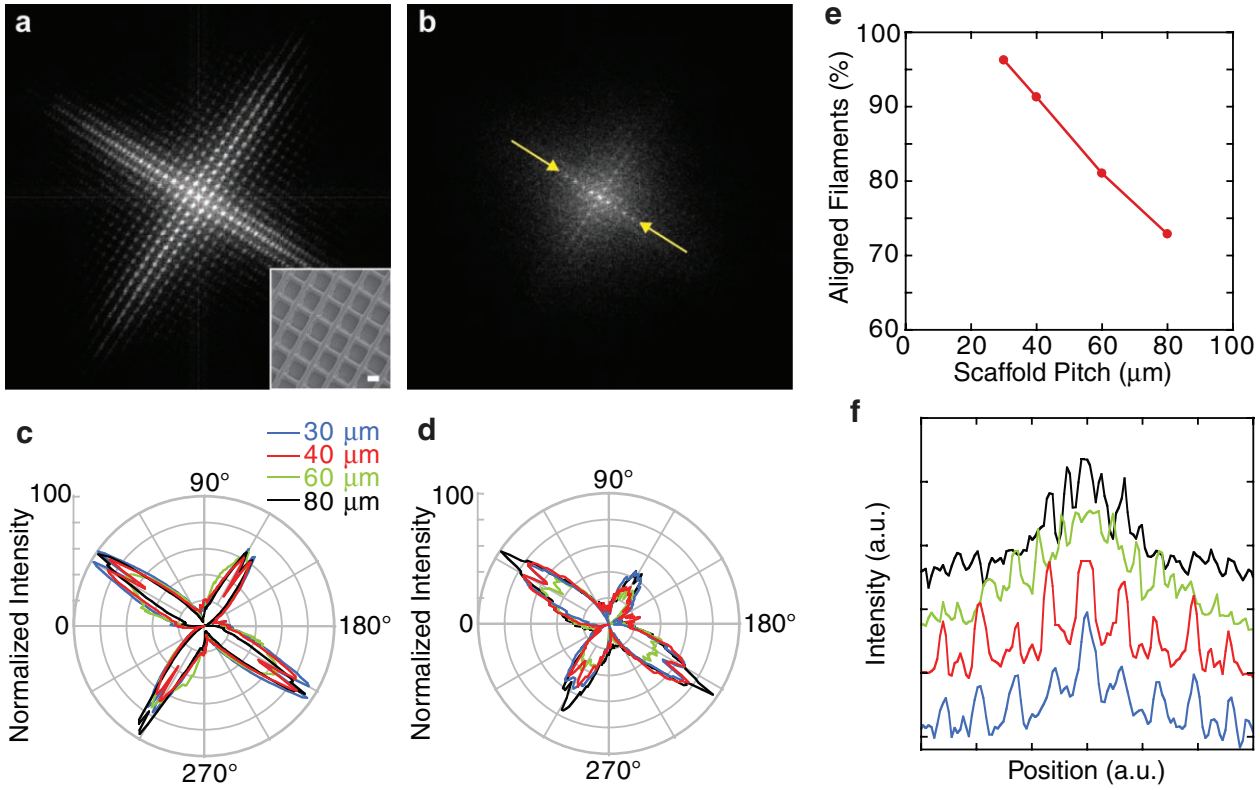

Figure 6. Planar representations of 3D fast Fourier transform (FFT) calculated for (a) scaffold with 40 μm pitch and (b) corresponding neuronal processes on this scaffold. Inset in (a) is an SEM image that indicates scaffold orientation. Normalized intensity as a function of angle for (c) scaffolds of varying pitch and (d) neuronal processes calculated from the FFTs. (e) Extent of process alignment as a function of scaffold pitch. (f) Line scans of intensity measured across the primary angle of the neuronal process alignment in the FFTs (denoted by arrows in (b)). Scale bar, 20 μm.

the two perpendicular scaffold orientations is observed on all scaffold architectures. An example of this is given in Figure 5d, where the neuronal processes of a soma in a 30 μm pitch scaffold are clearly guided by the patterned features.

To quantify the neuronal process alignment, separate fast Fourier transforms (FFT) are calculated for both the scaffolds and processes observed in the 3D reconstructed images. FFTs acquired from a 3D scaffold (40 μm pitch) and corresponding neuronal processes, shown in **Figure 6**a,b, reveal the strong periodicity of both the scaffold and the interacting neuronal processes. The inset in Figure 6a denotes the scaffold orientation. These images are analyzed and plotted for the specific rod and process fluorescence intensities as a function of angle (Figure 6c,d). The similarities between the two polar plots indicate that the neuronal processes have a similar degree of periodicity as the scaffolds, signifying that the processes closely follow along the topography of the scaffold. The anisotropy of this process alignment on the scaffolds can be approximated from the 3D reconstructions, as shown in Figure 6e. As expected, the correlation length of this induced anisotropy decreases as the pitch size increases. The intensity line scans taken across the primary angle in the neuronal process FFTs, shown in Figure 6f, indicates that the processes exhibit a higher degree of periodicity within 3D scaffolds of smaller pitch (i.e., 30–40 μm). Interestingly, scaffolds with 40 μm pitch present a better peak-to-noise ratio than those of 30 μm pitch. This may be due to the increased proclivity for processes to form bridges that span between rods in scaffolds of finer pitch, as illustrated in Figure 3a.

3. Conclusions

3D microperiodic hydrogel scaffolds have been developed that offer a robust, biocompatible culture system for primary hippocampal neurons. Using confocal microscopy coupled with image analysis, cell-scaffold interactions were observed and quantified in three dimensions providing insight to neuronal development in complex 3D environments. This programmable platform offers new opportunities for 3D *in vitro* studies of hippocampal neurons, as well as other sensitive cell types and tissues.

4. Experimental Section

Ink Design and Characterization: Hydrogel inks with varying concentrations of high molecular weight (M_w) pHEMA chains, HEMA monomer, ethylene glycol dimethacrylate (EGDMA) comonomer, dimethoxy-2-phenylacetophenone (DMPA) photoinitiator, and deionized water are created to identify the optimal formulation for direct-write assembly. Each ink is produced by combining appropriate amounts of HEMA, EGDMA, DMPA, and deionized water and stirred until the DMPA dissolves. Next, pHEMA chains of varying M_w and concentration are added to this mixture, which is then stirred for 48–72 h until a homogenous solution forms. The rheological properties of each ink are characterized, followed

by printing to assess its suitability for direct writing of 3D microperiodic scaffolds. The full results of these experiments will be reported elsewhere. From this process, we identified an optimal ink formulation composed of 25 wt% pHEMA (300,000 M_w), 10 wt% pHEMA (1,000,000 M_w), 40 wt% HEMA, 23.5 wt% H_2O, 1 wt% ethylene glycol dimethacrylate (EGDMA), and 0.5 wt% 2,2-dimethoxy-2-phenylacetophenone (DMPA) (Sigma) for patterning 3D scaffolds of interest.

The rheological properties of this pHEMA ink are determined using a controlled stress rheometer (Bohlin CVO Rheometer, Malvern Instruments Ltd., Worcestershire, UK) fitted with a cone and plate geometry (CP 4/40, cone diameter of 40 mm with a 4° angle and gap width of 150 μm). Shear viscosity measurements are carried out in controlled shear stress (τ) mode in a logarithmically ascending series of discrete steps. The elastic shear (G') and viscous (G'') moduli are measured using an oscillatory logarithmic stress sweep at a frequency of 1 Hz. Measurements are carried out at 22 °C using an aqueous solvent trap to mitigate drying effects.

Scaffold Fabrication: 3D pHEMA scaffolds are printed onto glass substrates (12 mm diameter, 0.17 mm thickness, Warner Instruments) that are piranha cleaned and soaked in a 5% 3-(Trimethoxysilyl) propyl methacrylate (Sigma) in toluene solution at 60 °C overnight and rinsed with isopropanol. Each scaffold is patterned using a 3-axis micropositioning stage (ABL9000, Aerotech Inc.) controlled by customized software (3D Inks). The ink is housed in a syringe (3 mL, EFD Inc.) mounted on the stage and extruded through a tapered micronozzle (10 μm, World Precision Instruments) onto the prepared substrates under an applied pressure of 100–200 kPa (800 Ultra dispensing system, EFD Inc.) at a speed of 200 μm s^{-1}. After patterning the initial layer, the nozzle is incrementally raised in the *z*-direction to generate the next layer, and repeated until the desired 3D scaffold architecture is formed.

After printing, each scaffold is exposed to UV light (OmniCure S2000, Exfo) for ~20 min and soaked in deionized water for at least 12 h to remove any unreacted species. The scaffolds are printed with 6 layers with overall dimensions ranging from 1×1 mm^2 to 1.16×1.16 mm^2. The center-to-center separation distance (or pitch) between pHEMA filaments ranges from 30–80 μm. SEM images of 3D unseeded pHEMA scaffolds are taken with a Hitachi S-4700 SEM after coating samples with gold/palladium for 45 s (Emitech K575 Sputter Coater).

Hippocampal Neuron Culture: The cell plating procedure is modified slightly from our previous study.[8] Prior to use in culture, pHEMA scaffold samples are sterilized for 20 min with UV, treated with poly-D-lysine (MW: 30–70 kDa, Sigma) at 100 μg/mL for 1 h, and then allowed to sit for 1 h. Hippocampal neurons are isolated from post-natal day one (P1) Long Evans/BluGill rats (University of Illinois-Urbana Champaign). All experiments are conducted under protocols approved by the UIUC Institutional Animal Care and Use Committee of the Vice Chancellor for Research, and under continuous supervision of the campus veterinarian staff. The brains are removed, the hemispheres separated, and the hippocampi dissected. Dissected tissue is kept in a 35 mm petri dish, surrounded by ice and filled with cold Hibernate A base solution (BrainBits), supplemented with 2% B-27 (Invitrogen) and L-glutamine (0.5 mM, Sigma). Upon completion of dissection, the tissue is incubated with Papain enzyme (2mg/mL, Worthington) at 37 °C for 15 min and then rinsed with 2 mL Hibernate A solution. The solution is removed, an additional 2 mL of Hibernate is added, and then the tissue is triturated approximately 10 times. After allowing the large pieces of tissue to settle, the cell solution is collected. This step is repeated at least once. The cell solution is centrifuged for 5 min at 3G and then reconstituted with 0.5 mL of Neurobasal base solution (Gibco), supplemented with 2% B-27 (Invitrogen), L-glutamine (0.5 mM), and 1% pen-strep (Sigma). The remaining large chunks of tissue are incubated again with papain enzyme (2 mg/mL) for 15 min and the above process is repeated. Once the incubation time is complete, the cell suspensions are combined and used to plate the scaffold substrates at an initial density of approximately 500 cells/mm^2. The neurons are maintained in a humidified environment at 37 °C with 5% CO_2 and supplemented with Neurobasal media twice weekly for one week.

Immunocytochemistry – Actin/Nucleus Staining: After 7 days in culture, neurons are rinsed 3 times with PBS, immersed in 4% paraformaldehyde at room temperature for 30 min and then rinsed again with PBS, 2×. A PBS solution containing 0.1% Triton X-100 is placed on the samples for 15 min to permeablize cellular membranes, before rinsing again with PBS (0.1% Tween),. The samples are then incubated in ITsignal FX (Invitrogen Molecular Probes) for 30 min and then rinsed briefly with PBS (0.1% Tween). Samples are incubated in a 1:100 solution (with PBS and 100 μl of ITsignal FX) of mouse anti-actin monoclonal antibody (MP Biomedicals, Solon, OH) for 2 h and then rinsed with PBS (0.1% Tween), 3× (5 min). Cells are incubated for 1 h with a secondary antibody, Goat Anti-Mouse Alexa 568 (Invitrogen Molecular Probes) in a 1:200 dilution (with PBS and 100 μl of ITsignal FX) in the dark. Samples are rinsed with PBS (0.1% Tween), 3× (5 min) and then exposed to TO-PRO3 (Invitrogen Molecular Probes) at 5 μM in PBS, for 30 min in the dark. Once the exposure is complete, the samples are rinsed briefly with PBS (Tween 0.1%) and then mounted in Prolong Gold (Invitrogen). Samples are sealed after 24 h and kept covered, at 4 °C until imaged. Note, samples from 4 different *in-vitro* experiments are stained using this protocol and analyzed. Details on MAP2 staining can be found in the Supporting Information.

Confocal Imaging: Confocal images are acquired using a Zeiss LSM 710 multi-photon confocal microscope. Tiled images of the entire scaffold are obtained using the 25× objective, which are composed of either 3×3 tiles (927 μm × 927 μm) or 4×4 tiles (1270 μm × 1270 μm) depending on the scaffold architecture. In addition, 2×2 tiled images (250 μm × 250 μm) are captured using a 40× objective for data analysis purposes.

Image Analysis: Confocal *z*-stacks are reconstructed using Imaris software (Bitplane, Inc.). The distribution of cells is determined using the Spots Analysis. At least two samples, from different culture dates, are analyzed for each scaffold architecture. Position data is imported into MATLAB (The MathWorks) and viewed in 3D from the *x*-*z* plane, in which cell size is varied to indicate its position along the *y*-axis.

Scaffold and neuronal process *z*-stacks are reconstructed into separate 3D arrays using MATLAB. A Multidimensional Fast Fourier Transform (FFT) package is used to analyze the 3D arrays. The function 'fftn' is used to determine the 3D FFT; 'fftshift' is then used to center the low frequency components of the transform. The power spectrum is taken as the log of the absolute value of the centered transform and scaled identically between samples to display in the grayscale color range 0 to 255. In order to determine the orientation of the neuronal processes, the 'fanbeam' function is used to integrate around the lateral (*x*-*y*) and vertical (*x*-*z*) orientations, in which the lateral orientation possesses the highest intensity. Only the center beam of the 'fanbeam' projection is used in a 360° rotation. A low pass filter is used on each FFT image to remove the lowest value, and then the data is normalized. Intensity linescans are taken across the primary angle in the process FFT images using ImageJ (U.S. NIH). Dilated scaffold 3D arrays are subtracted from the process 3D arrays to calculate the percent of the neuronal network on the scaffold.

Acknowledgements

J.N.H.S. and S.T.P. contributed equally to this work. The authors thank K. Weis for assistance with cell culture and M. Sivaguru for discussion on confocal imaging. We acknowledge the UIUC IGB Core Facilities for use of the LSM 710. This work was supported by the National Science Foundation (Grant# CHE0704153 and Grant# DMR0652424), the National Institutes of Health (Grant# MH085220 and R01 EY01736–01A1), and the NSF Center for Nanoscale Chemical-Electrical-Mechanical Manufacturing Systems (DMI-0328162).

Competing Financial Interests

This work has been disclosed to the Office of Technology Management at the University of Illinois-Urbana Champaign and a patent application has been submitted.

Received: August 23, 2010
Published online: November 12, 2010

[1] R. P. Lanza, R. Langer, J. P. Vacanti, *Principles of Tissue Engineering*, Elsevier Science, **1997**.
[2] R. Langer, J. Vacanti, *Science* **1993**, *260*, 920.
[3] E. Cukierman, R. Pankov, D. R. Stevens, K. M. Yamada, Science **2001**, *294*, 1708.
[4] M. Schindler, A. Nur-E-Kamal, I. Ahmed, J. Kamal, H.-Y. Liu, N. Amor, A. Ponery, D. Crockett, T. Grafe, H. Chung, T. Weik, E. Jones, S. Meiners, *Cell Biochem. Biophys.* **2006**, *45*, 215.
[5] M. F. Bear, B. W. Connors, M. A. Paradiso, *Neuroscience: Exploring the Brain*, Lippincott Williams & Wilkins, Philadelphia **2007**.
[6] A. M. Rajnicek, S. Britland, C. D. McCaig, *J. Cell Sci.* **1997**, *110*, 2905.
[7] N. M. Dowell-Mesfin, M.-A. Abdul-Karim, A. M. P. Turner, S. Schanz, H. G. Craighead, B. Roysam, J. N. Turner, W. Shain, *J. Neural Eng.* **2004**, *1*, 78.
[8] J. N. Hanson, M. J. Motola, M. L. Heien, M. Gillette, J. V. Sweedler, R. G. Nuzzo, *Lab Chip* **2009**, *9*, 122.
[9] P. Clark, S. Britland, P. Connolly, *J. Cell Sci.* **1993**, *105*, 203.
[10] A. Offenhaeusser, S. Boecker-Meffert, T. Decker, R. Helpenstein, P. Gasteier, J. Groll, M. Moeller, A. Reska, S. Schaefer, P. Schulte, A. Vogt-Eisele, *Soft Matter* **2007**, *3*, 290.
[11] L. Kam, W. Shain, J. N. Turner, R. Bizios, *Biomaterials* **2001**, *22*, 1049.
[12] Y. Luo, M. S. Shoichet, *Nat. Mater.* **2004**, *3*, 249.
[13] C. E. Schmidt, J. B. Leach, Annu. *Rev. Biomed. Eng.* **2003**, *5*, 293.
[14] S. M. Willerth, K. J. Arendas, D. I. Gottlieb, S. E. Sakiyama-Elbert, *Biomaterials* **2006**, *27*, 5990.
[15] T. C. Holmes, S. de Lacalle, X. Su, G. Liu, A. Rich, S. Zhang, *Proc. Natl. Acad. Sci USA* **2000**, *97*, 6728.
[16] H. R. Irons, D. K. Cullen, N. P. Shapiro, L. N. A. R. H. Lee, M. C. LaPlaca, *J. Neural Eng.* **2008**, 333.
[17] K. Moore, M. MacSween, M. Shoichet, *Tissue Eng.* **2006**, *12*, 267.
[18] S. K. Seidlits, C. E. Schmidt, J. B. Shear, *Adv. Funct. Mater.* **2009**, *19*, 3543.
[19] G. M. Gratson, M. Xu, J. A. Lewis, *Nature* **2004**, *428*, 386.
[20] J. A. Lewis, *Adv. Funct. Mater.* **2006**, *16*, 219.
[21] R. A. Barry III, R. F. Shepherd, J. N. Hanson, R. G. Nuzzo, P. Wiltzius, J. A. Lewis, *Adv. Mater.* **2009**, *21*, 2407.
[22] J. Bruneaux, D. Therriault, M. Heuzey, J. Micromech. *Microeng.* **2008**, *18*, 115020.
[23] G. J. Brewer, *J. Neurosci. Meth.* **1997**, *71*, 143.
[24] J. Ray, D. A. Peterson, M. Schinstine, F. H. Gage, *Proc. Natl. Acad. Sci USA* **1993**, *90*, 3602.